Structure and Phases of the Au(001) Surface: X-Ray Scattering Measurements

S. G. J. Mochrie
Physics Department, Massachusetts Institute of Technology, Cambridge, Massachusetts 02139

D. M. Zehner
Solid State Division, Oak Ridge National Laboratory, Oak Ridge, Tennessee 37831

B. M. Ocko and Doon Gibbs
Physics Department, Brookhaven National Laboratory, Upton, New York 11973
(Received 6 December 1989)

X-ray diffraction is used to study the phase behavior and structure of the Au(001) surface between 300 K and the triple point. For $T > 1170$ K, the x-ray reflectivity is consistent with a thin, disordered surface film. At 1170 K, there is a reversible transition to an incommensurate, hexagonal overlayer on top of the square substrate. At 970 K, the orientation of the hexagonal layer rotates discontinuously by 0.81° with no observable change in incommensurability.

PACS numbers: 68.35.Rh, 61.10.−i, 64.70.Dv

The Au(001) surface exhibits a novel reconstruction in which the topmost layer of atoms is believed to form a near hexagonal lattice on top of the subsequent planes of square symmetry. In spite of this appealingly simple picture, a completely consistent description of the room-temperature structure has yet to emerge.[1-5] Much less is known about the behavior at higher temperatures,[6] but one can anticipate that a temperature-dependent study of this surface will provide insights into two-dimensional structures and phase transitions. In addition, experiments at temperatures near bulk melting are essential for an understanding of the global stability of crystal surfaces, and of the relationships between such phenomena as roughening transitions, enhanced surface vibrations, and surface and bulk melting. Accordingly, we have carried out a comprehensive x-ray diffraction study of the clean Au(001) surface between 300 K and just below the triple point ($T_t = 1337$ K). Our results encompass a variety of behavior including a rotational transition and a surface-disordering transition. They also provide a detailed three-dimensional description of the surface structure. In this Letter, we present a summary of the results; a complete account of the experimental procedures, data, and analysis is given in Refs. 7 and 8.

Experiments on the clean Au(001) surface, performed in an ultrahigh-vacuum environment,[6-8] were carried out at beam line A2 at the Cornell High Energy Synchrotron Source and at the National Synchrotron Light Source using beam lines X22C, X20C, and X22B. For large incidence angles (α), slits were used to define the illuminated sample area and all scattered x rays were collected. Then, the reflectivity from a given surface periodicity (τ_x, τ_y) is[6,8]

$$R = \left(\frac{4\pi r_0}{c^2 k \sin\alpha}\right)^2 |F(\mathbf{Q})|^2 e^{-2W(\mathbf{Q})} \left|\sum_{n=0}^{\infty} \rho_{\mathbf{Q}}(n) e^{iQ_z cn/2}\right|^2, \quad (1)$$

where $\mathbf{Q} = (\tau_x, \tau_y, Q_z)$ is the wave-vector transfer, r_0 is the Thomson radius, $F(\mathbf{Q})$ is the form factor, $W(\mathbf{Q})$ is the Debye-Waller factor, c is the cubic lattice constant of Au, and $\rho_{\mathbf{Q}}(n)$ is the amplitude of the density wave in the nth layer. We will discuss specific forms for $\rho_{\mathbf{Q}}(n)$ below. However, it is important to note that R need not depend on instrumental parameters, so that absolute measurements are possible. At grazing incidence, a Ge(111) analyzer was employed for fine resolution measurements of the overlayer lattice constants and rotation angle.

Figures 1(a)–1(c) depict the $(H,K,0)$ plane of reciprocal space for each of the three phases that we have observed. Each symbol represents a rod of scattering extending normal to the surface. Thus, specular reflectivity corresponds to $\tau_x = \tau_y = 0$; nonspecular to $\tau_x, \tau_y \neq 0$. The high-temperature phase between T_t and 1170 K is shown in Fig. 1(a). There is no scattering associated with lateral periodicities different from those of the bulk (001) planes (solid squares). More importantly, the Q_z dependence of the reflectivity is consistent with a thin disordered or liquid surface film[9] (1–2 layers) and not with an ideally terminated crystal. At 1170 K, the topmost layer undergoes a reversible transition into an incommensurate, distorted-hexagonal phase [open triangles in Fig. 1(b)]. An important feature of this structure is an incommensurate corrugation along the cubic [110] direction with a wave vector (δ) just equal to the difference between overlayer $(1,0)h$ and substrate $(1,1,0)c$ wave vectors. In Au reciprocal-lattice units $\delta = (0.206 \pm 0.001)\sqrt{2}c^*$ ($c^* = 2\pi/c$, where $c = 4.08$ Å at 300 K). This gives rise to satellites (solid circles) along directions parallel to the [110] direction, about each hexagonal position. The existence of the satellites at 300 K led to earlier descriptions of the surface as having a (5×1) reconstruction. The incommensurability in the $[1\bar{1}0]$ direction is $(0.043 \pm 0.001)\sqrt{2}c^*$, but there are no corresponding satellite peaks. At 970 K, the topmost layer undergoes a

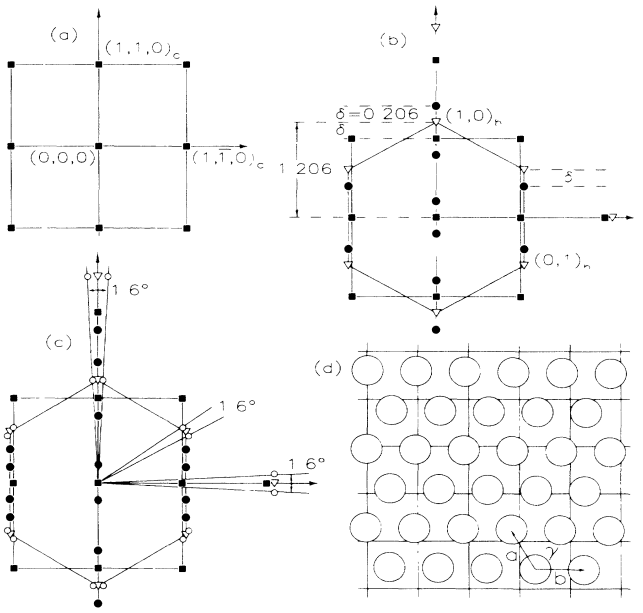

FIG. 1. $(H,K,0)$ plane of reciprocal space for (001) surface of Au. (a) Disordered phase; (b) distorted-hexagonal phase; (c) rotated, distorted-hexagonal phase; (d) illustration of the structure of the rotated, distorted-hexagonal phase: $a=2.765\pm0.002$ Å, $b=2.766\pm0.002$ Å, $\gamma=120.03\pm0.05°$. The [110] and [1$\bar{1}$0] directions indicated in (a) also apply to (b), (c), and (d).

rotational transmission at which domains rotate discontinuously by $\pm0.81°$ with no observable change in the incommensurability [Fig. 1(c)]. Figure 1(d) illustrates the structure of this phase. On further cooling the rotation angle and incommensurability are only weakly temperature dependent; however, aligned domains always remain in coexistence with the rotated domains. At all temperatures, the vibrational amplitude normal to the surface in the top few layers is substantially enhanced above the bulk value. While previous studies have suggested individual components of the room-temperature structure, such as the possibility of an incommensurate overlayer,[2,3] rotated domains,[3,4] and a surface corrugation,[5] one purpose of this Letter is to point out the straightforward manner in which all of these details, as well as others, emerge from x-ray measurements. In this regard, we note several recent theoretical studies of the Au(001) surface.[10]

Figure 2 displays the measured absolute reflectivity as a function of $L=Q_z c/2\pi$ at a temperature of 1100 K, for several in-plane wave vectors. Because the data extend over a large range to $Q_z\cong5$ Å^{-1}, they are particularly sensitive to atomic coordinates perpendicular to the surface, and allow detailed modeling of the surface structure. Each point represents the integrated intensity obtained in a transverse scan.[6] The specular reflectivity is plotted in Fig. 2, curve *a*. As has been discussed previously,[6] the line-shape asymmetry about the Bragg peak

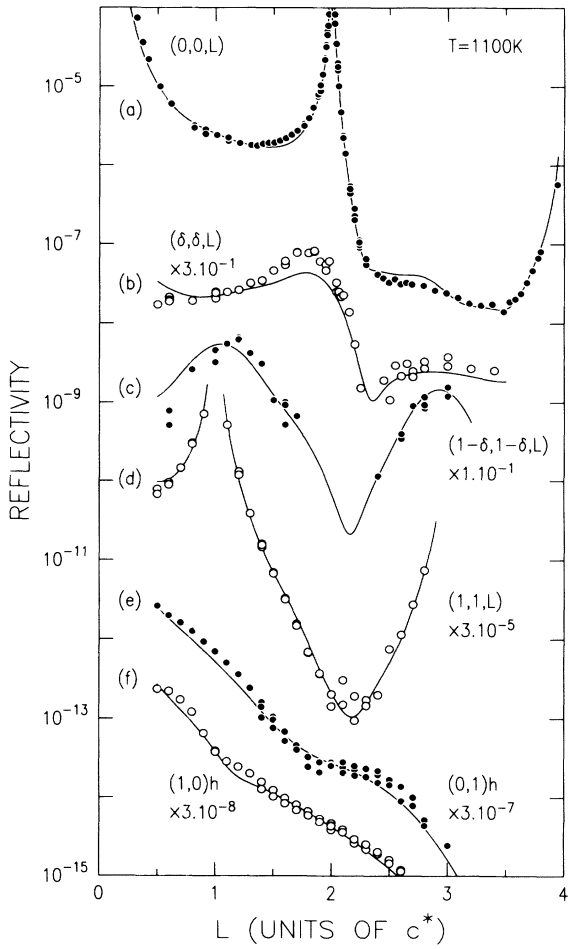

FIG. 2. Absolute reflectivity of Au(001) at 1100 K for various different in-plane wave-vector transfers (τ_1,τ_1): curve *a*, (0,0), specular reflectivity; curve *b*, (δ,δ); curve *c*, $(1-\delta, 1-\delta)$; curve *d*, (1,1); curve *e*, $(0,1)h$; and curve *f*, $(1,0)h$.

is a clear signature of a top-layer expansion [$d_{01}=1.19\times(c/2)$]. Figure 2, curves *e* and *f*, show the nonspecular reflectivity at the principle hexagonal wave vectors, $(1,0)h$ and $(0,1)h$. Qualitatively, the Q_z dependence follows the $(\sin\alpha)^{-2}$ behavior expected from Eq. (1) for a hexagonal monolayer. The small deviations are related to the surface corrugation and small displacements parallel to [1$\bar{1}$0].[8] Figure 2, curve *b*, shows the reflectivity at the modulation wave vector. This profile shows a significant increase from $L=1$ to 2 and a line-shape asymmetry about $L=2$, reminiscent of the specular reflectivity. This suggests that several layers participate in the reconstruction. There is, however, no increase near $L=0$, indicating that the modulation is a surface corrugation with the atomic displacements normal to the surface.

We have fitted the reflectivity results by Eq. (1), assuming a locally commensurate (5×1) structure. While this motif is not repeated periodically, nevertheless, such a simple model for $\rho_Q(n)$ provides an excellent descrip-

TABLE I. The rms surface-normal vibrational amplitude for the nth layer (σ_n) vs temperature. The surface layer corresponds to $n=0$.

Temperature (K)	σ_0 (Å)	σ_1 (Å)	σ_2 (Å)	σ_3 (Å)	σ_4 (Å)	σ_5 (Å)	Bulk
300	0.19 ± 0.02	0.17	0.09	0.09	0.09	0.09	0.09
1100	0.32	0.26	0.22	0.19	0.17	0.17	0.17
1200	0.44 ± 0.04	0.34	0.29	0.24	0.21	0.19	0.18

tion of the data (solid lines in Fig. 2). The parameters used were a layer-dependent sinusoidal corrugation amplitude for layer n (ζ_0-ζ_5), the layer spacings (d_{01},d_{12}), and a layer-dependent vibrational amplitude *normal to the surface* (σ_0-σ_3). (We defer discussion of displacements along [1$\bar{1}$0] to Ref. 8.) Allowing parameters for additional layers to vary did not improve the quality of the fits. Fitting all of the profiles of Fig. 2 together confirms the expectations outlined above and describes in detail the data of Fig. 2, curves *c* and *d*. We find that the dependence of ζ_n on the distance from the surface (z_n) is well described by $\zeta_n=\zeta_0\exp(-z_n/\lambda)$ with $\zeta_0=0.28\pm0.02$ Å (0.56 Å peak-to-peak), in reasonable agreement with Ref. 5, and $\lambda=3.3\pm0.6$ Å. Simple elasticity theory leads one to expect that λ be of the order of the modulation wavelength divided by 2π, i.e., 2.29 Å. The surface-normal vibrational amplitudes approach the bulk value for large n but are enhanced near the surface (Table I). As for the interlayer spacings, only d_{01} is measurably different from the bulk layer spacing.

Transverse scans of the (1,0)h peak are shown in Fig. 3. At the highest temperatures ($T>970$ K), all of the intensity is aligned with the [110] direction ($\omega=0°$). As the temperature is lowered through 970 K additional scattering appears at $\omega=\pm0.81°$ and increases with decreasing temperature. Examination of all peaks [e.g., the (1,1)h and the (2,0)h] reveals that each is accompanied by peaks rotated by $\pm0.81°$. This establishes that there are regions on the surface that rotate discontinuously away from the high-symmetry direction by $\pm0.81°$. Between 300 K and the disordering temperature (1170 K), the incommensurability (in units of c^*) is only weakly temperature dependent.[7] The rotation angle likewise does not change between 980 and 300 K, but only in the aligned phase are the radial peak widths resolution limited FWHM$=0.0014c^*$.[7] Coexistence of the rotated and unrotated populations, as well as the excess peak widths, implies that the overlayer is not at true thermodynamic equilibrium. For increasing temperatures the scattering at $\pm0.81°$ disappears by 980 K and the peak width reproduces its high-temperature value. Thus, the rotational transition is reversible. The discontinuous change in rotation angle with temperature cannot easily be understood within the context of current theories[7,11] of orientational epitaxy which predict that the misfit determines a definite rotation angle.

At 1170 K, all scattering at the hexagonal and satellite positions vanishes abruptly, consistent with a first-order transition to an unreconstructed structure for $T>1170$ K. In addition, the reflectivity near (1,1,0) decreases by a factor of ~100.[7] To further examine the nature of the surface at high temperatures, we per-

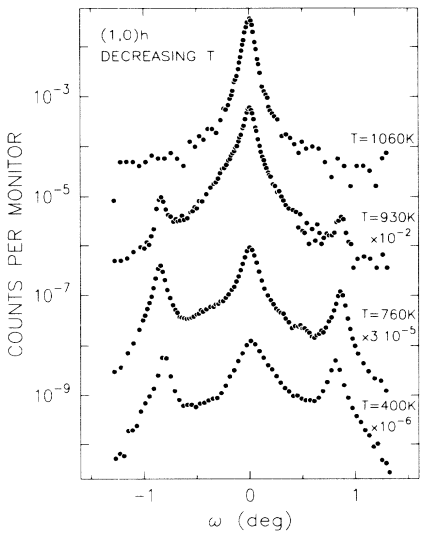

FIG. 3. Grazing incidence transverse scans through the (1,0)h peak for temperatures decreasing from 1060 to 400 K.

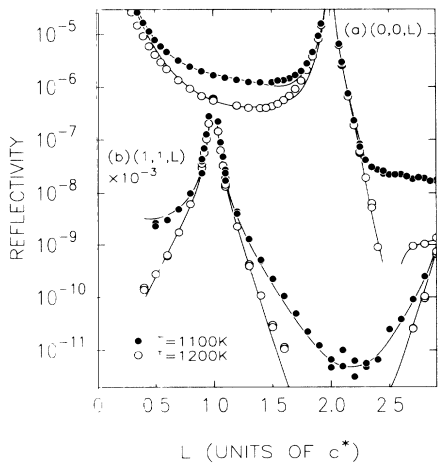

FIG. 4. Curve *a*, specular and, curve *b*, nonspecular reflectivity at 1100 K (closed circles) in the distorted-hexagonal phase and at 1200 K in the disordered phase (open circles).

formed measurements of the specular and nonspecular reflectivity near 1170 K. Examples are shown in Fig. 4, at 1200 K and, for comparison, at 1100 K in the distorted-hexagonal phase. Evidently, there is a dramatic change in going through the transition. In contrast, there is no change in the transverse line shape or position.[8] One can characterize the specular reflectivity as corresponding to an unreconstructed surface with enhanced surface-normal vibrational amplitudes. However, it is impossible on this basis alone to understand the decrease of the $(1,1,L)$ reflectivity at small L from 1100 to 1200 K. On the other hand, the reflectivity from a gradual interface is invariably less than that from a sharp interface.[8] Thus these data imply that at high temperatures the in-plane (1,1,0) cubic density wave decays as the surface is approached from the bulk. This, in fact, is the behavior expected if the surface undergoes surface melting.[12] To model the data of Fig. 4, we have chosen the following form for $\rho_G(n)$ [$\mathbf{G}=(110)$ cubic] in the disordered phase

$$\rho_G(n)/\rho_G(\infty)=1-1/[1+e^{-\kappa l}\sinh(\kappa n+S)], \quad (2)$$

with $S=e^{\kappa l}[1/(1-e^{-\kappa l})-1]$. Other parametrizations are also possible, for example, in terms of large in-plane vibrational amplitudes (larger than the surface-normal vibrational amplitudes). According to Eq. (2), the density-wave profile is described by two parameters: the width of the interface (κ^{-1}) and the thickness of the disordered, surface layer (l). The solid lines of Fig. 4 are the results of fits with a model which allows a surface-normal vibrational amplitude for each layer near the surface and which characterizes $\rho_G(n)$ via Eq. (2); the density of the surface layer was fixed equal to that of the bulk planes. The resultant values of κ^{-1} and l are 2.9 ± 0.4 Å and 3.2 ± 1.2 Å, respectively, and indicate that the surface may be described as one or two liquid-like layers at these temperatures. The best-fit value of d_{01} corresponds to an 8.5% expansion. The vibrational amplitudes, determined by the specular reflectivity, are given in Table I. Since the surface-normal vibrational amplitudes are less than the (001)-layer spacing, the layer order is still well established right to the surface.

In summary, we have presented a detailed x-ray diffraction study of the Au(001) surface. This has allowed a definitive characterization of the reconstruction. We have uncovered a rotational transition, which is not naturally described by current theories. Finally, we have presented evidence for a surface-disordering transition. Future experiments will study the behavior nearer the triple point and especially the thickness of the disordered layer.[9,12] It remains to determine whether surface disordering in this case is a consequence of the instability which leads to the reconstruction, or whether it is generic to fcc (001) metal surfaces.

We would particularly like to thank G. Ownby for technical assistance. Work at MIT is supported by the NSF (Grants No. DMR-8806591 and No. DMR-8719217), work at BNL by the DOE (Contract No. DE-AC0276CH00016), and at ORNL by the DOE (Contract No. DE-AC02840R21400). X20 is supported by the NSF Materials Research Laboratory Program MIT (Grant No. DMR-8719217) and by IBM.

[1]D. M. Zehner, B. R. Appleton, T. S. Noggle, J. W. Miller, J. H. Barret, L. A. Jenkins, and E. Schow, III, J. Vac. Sci. Technol. **12**, 454 (1975).

[2]M. A. Van Hove, R. J. Koestner, P. C. Stair, J. B. Biberian, L. L. Kesmodel, I. Bartos, and G. A. Somarjai, Surf. Sci. **103**, 189 (1981).

[3]G. Binnig, H. Rohrer, Ch. Gerber, and E. Stoff, Surf. Sci. **144**, 321 (1984).

[4]K. Yamazaki, K. Takayanagi, Y. Tanishiro, and K. Yagi, Surf. Sci. **199**, 595 (1988).

[5]K. H. Rieder, T. Engel, R. H. Swendsen, and M. Manninen, Surf. Sci. **127**, 223 (1983).

[6]D. Gibbs, B. M. Ocko, D. M. Zehner, and S. G. J. Mochrie, Phys. Rev. B **38**, 7303 (1988).

[7]D. Gibbs, B. M. Ocko, D. M. Zehner, and S. G. J. Mochrie (unpublished).

[8]B. M. Ocko, D. Gibbs, K. Huang, D. M. Zehner, and S. G. J. Mochrie (unpublished).

[9]See, for example, J. W. M. Frenken, P. M. J. Marée, and J. F. van der Veen, Phys. Rev. B **34**, 7506 (1986).

[10]F. Ercolessi, E. Tosatti, and M. Parinello, Phys. Rev. Lett. **57**, 719 (1986); B. W. Dodson, Phys. Rev. B **35**, 880 (1987); N. Takeuchi, C. T. Chan, and K. M. Ho, Phys. Rev. Lett. **63**, 1273 (1989).

[11]J. P. McTague and A. D. Novaco, Phys. Rev. B **19**, 5299 (1979); J. Villain, Phys. Rev. Lett. **41**, 36 (1978); H. Shiba, J. Phys. Soc. Jpn. **46**, 1852 (1979); **48**, 211 (1980).

[12]R. Lipowsky and W. Speth, Phys. Rev. B **28**, 3938 (1983).